Supplementary material

Table S1. INP levels, precipitations, snow depth and land type contact data for the October – November 2019 campaign. The division in three periods of the campaign refers to the considerations done in Sect. 3.3.

Period	Date	*n*INP T = -22°C	*n*INP T = -18°C	*n*INP T = -15°C	Cumulative precipitation (mm)	Snow depth (cm)	Contact with Sea Water (%)	Contact with Sea Ice (%)
1	Up to 16/10	75.8	29.0	11.0	6.1	0.0	68.6	1.1
2	From 17/10 to 08/11	64.7	27.1	6.3	9.8	3.0	28.4	55.6
3	From 09/11	39.5	20.3	3.1	25.4	16.5	42.7	28.1

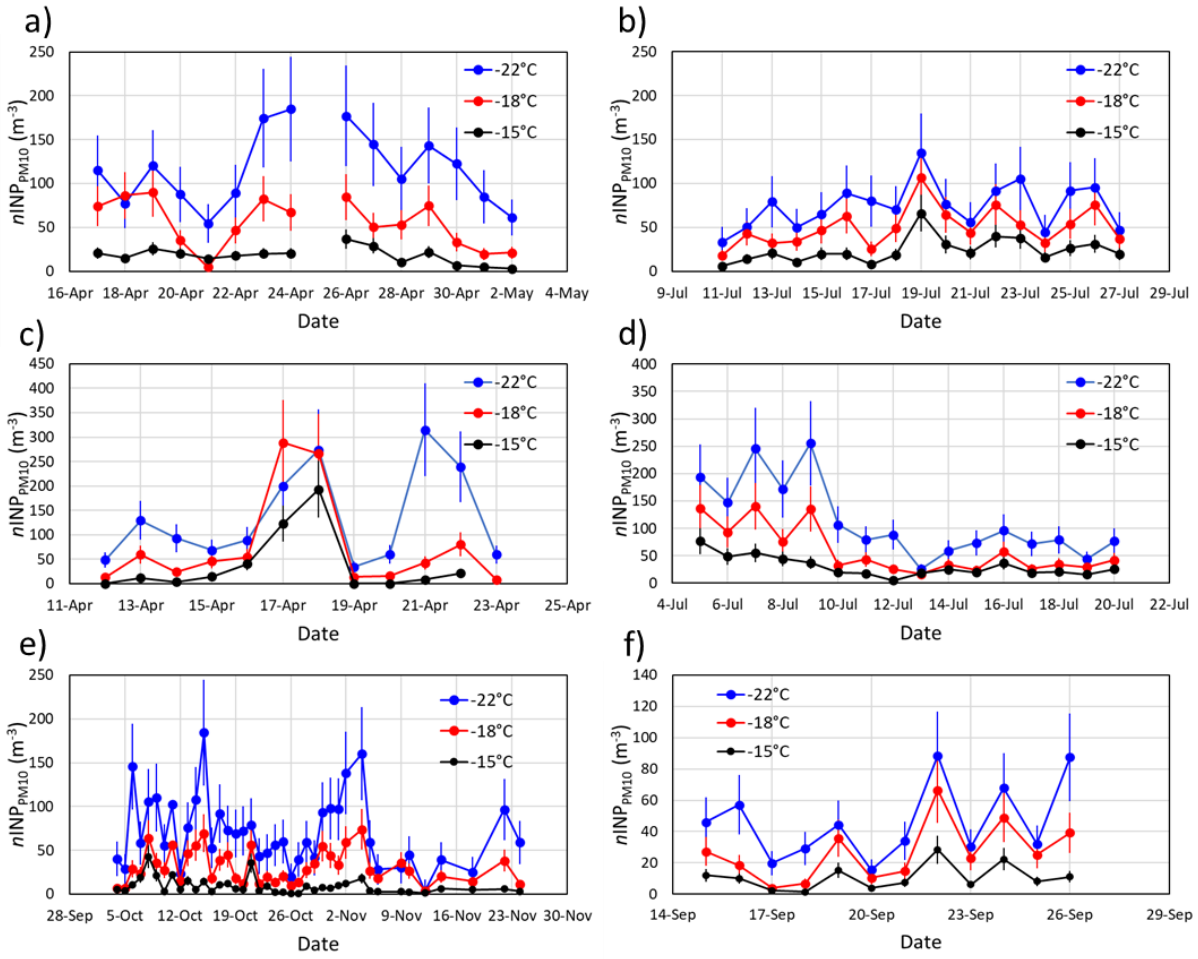

Figure S1. *n*INP, in the PM_{10} size range, measured during the (a) spring 2018, (b) summer 2018, (c) spring 2019, (d) summer 2019, (e) autumn 2019 and (f) autumn 2020 campaign.

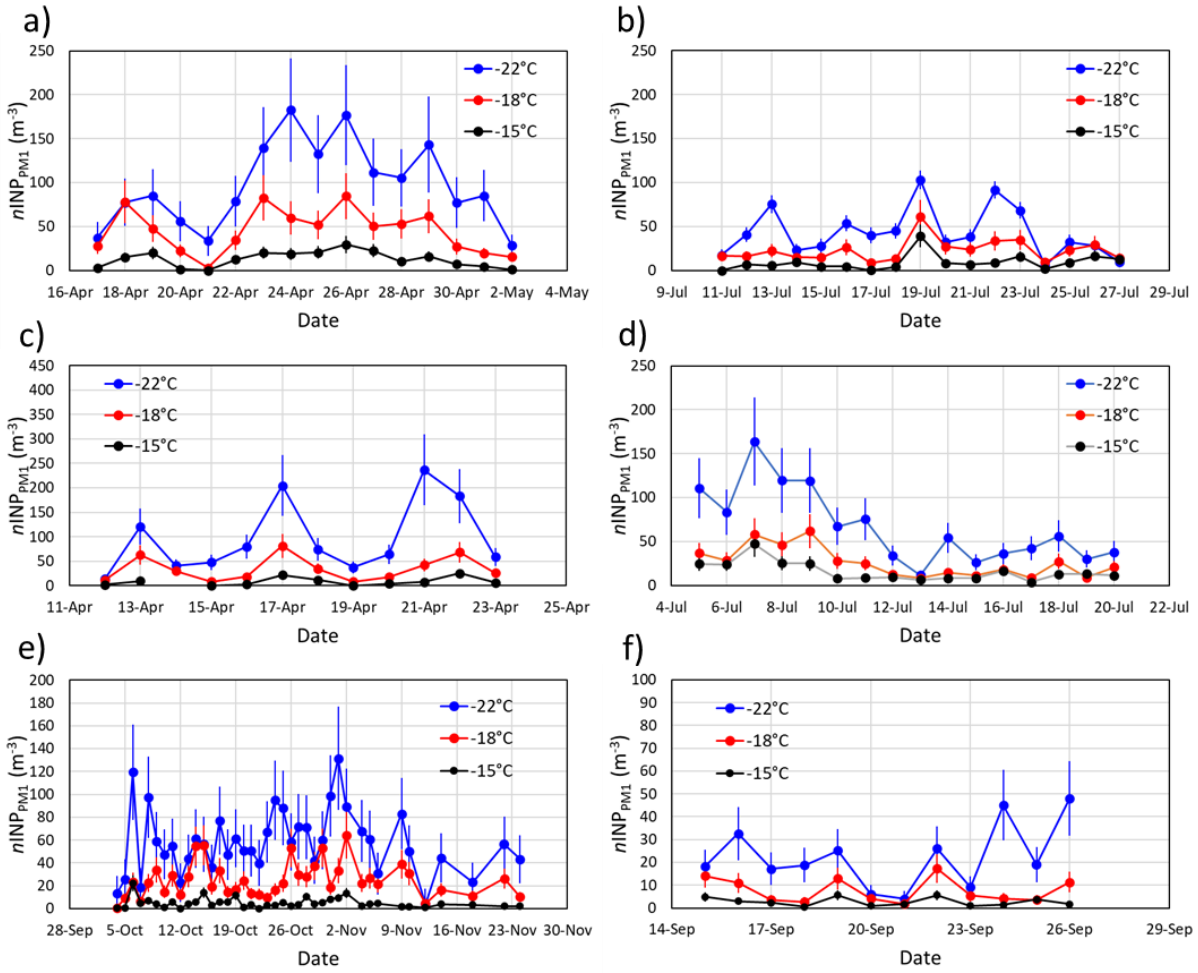

Figure S2. *n*INP, in the PM_1 size range, measured during the (a) spring 2018, (b) summer 2018, (c) spring 2019, (d) summer 2019, (e) autumn 2019 and (f) autumn 2020 campaign.

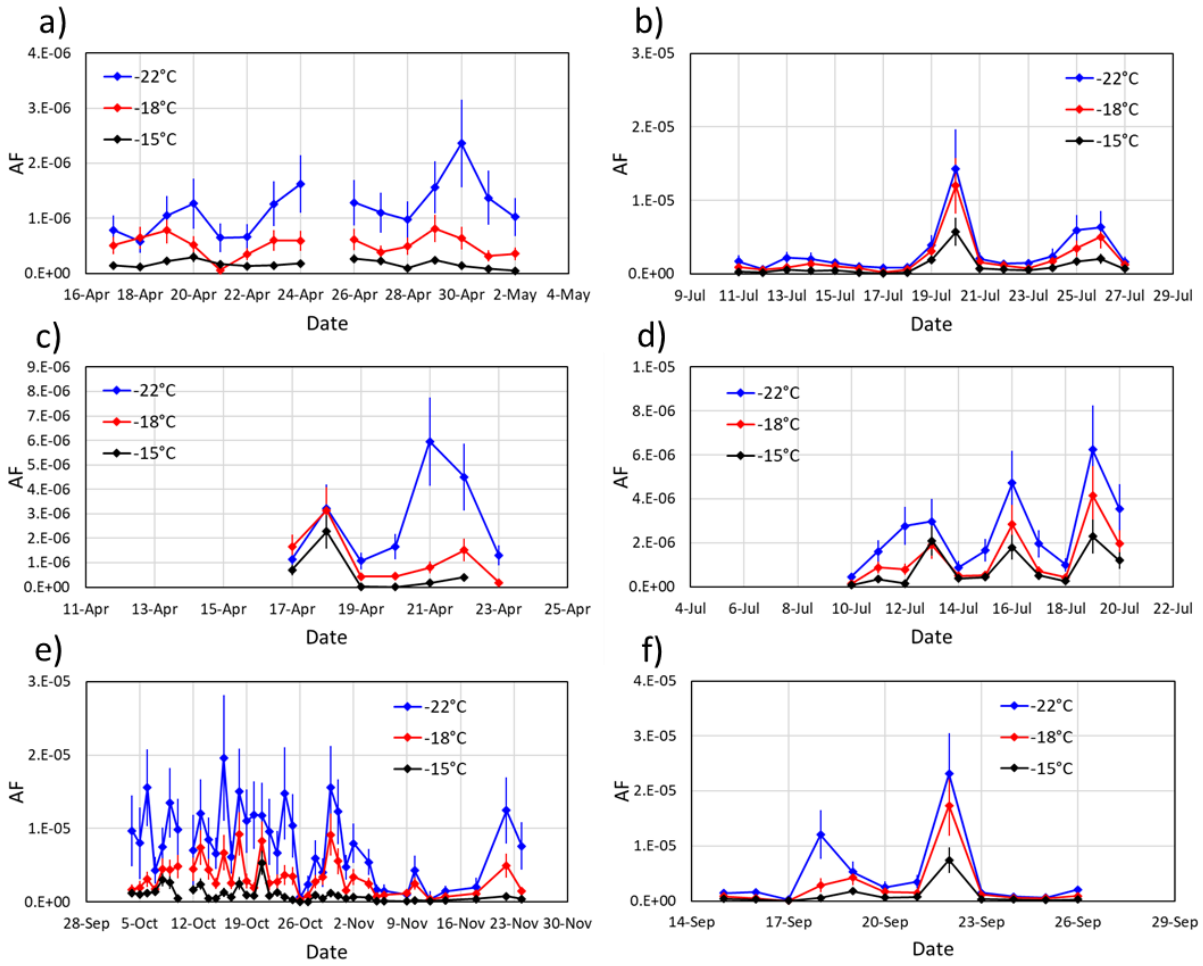

Figure S3. AF, in the PM_{10} size range, measured during the (a) spring 2018, (b) summer 2018, (c) spring 2019, (d) summer 2019, (e) autumn 2019 and (f) autumn 2020 campaign. Missing AF data in (c) and (d) are due to unavailable particle number concentration data.

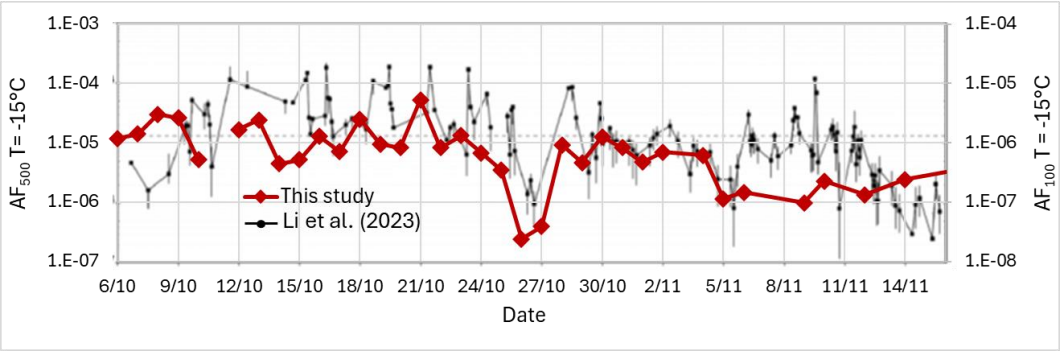

Figure S4. AF_{500} (referring to the 0.5-10 µm particle number concentration; right axis) and AF_{100} (referring to the 0.1-10 µm particle number concentration; left axis) calculated for T = -15°C in the present study and by Li et al. (2023) for parallel measurements performed at GVB.

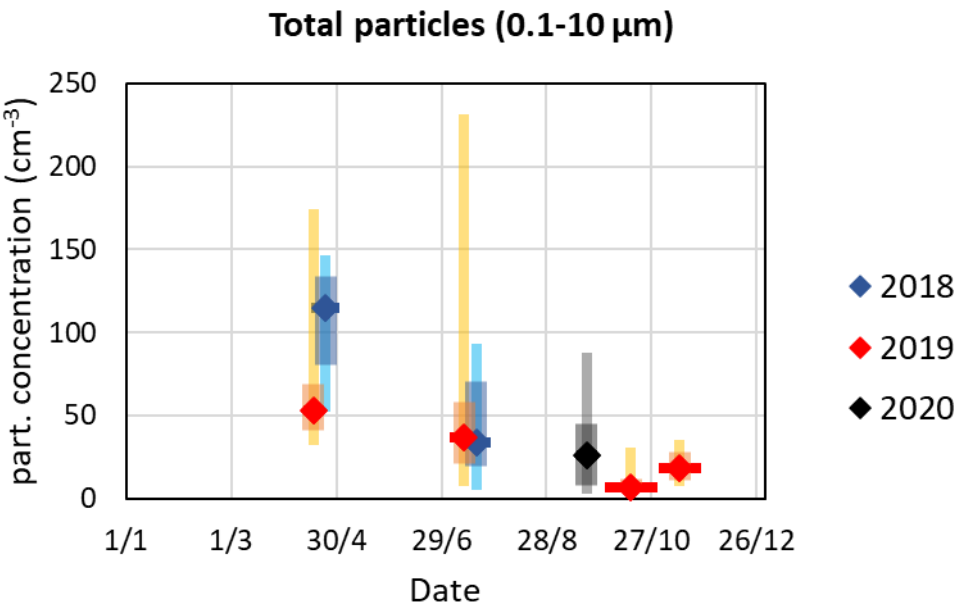

Figure S5. Seasonal variation of the particle number concentration in the 0.1 – 10 µm size range. The diamonds indicate the median values, while the vertical thicker and thinner bars represent the interquartile range and the min-max range, respectively. The horizontal bars indicate the time span of each measurement period.

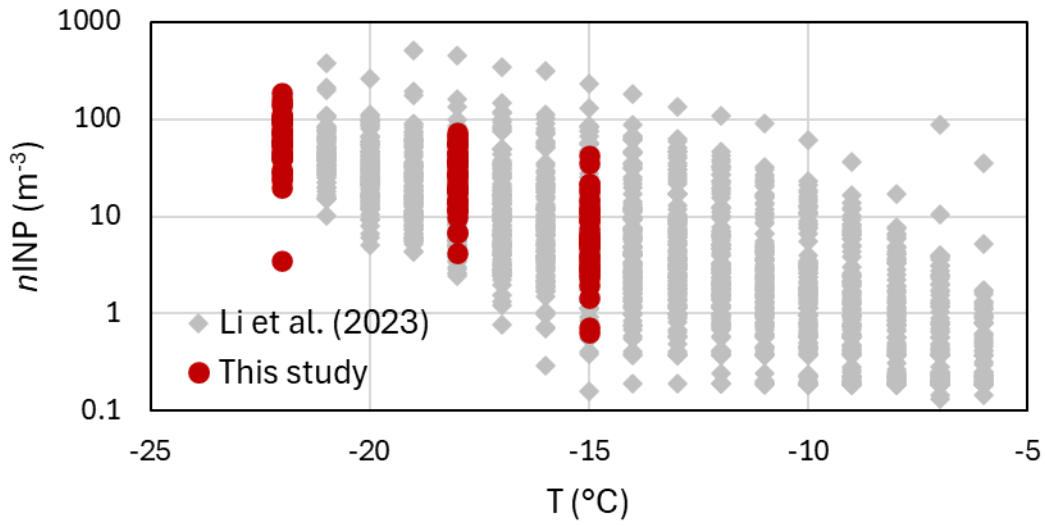

Figure S6. *n*INP as a function of T measured at GVB during autumn 2019. Data from Li et al. (2023) were obtained by immersion freezing.

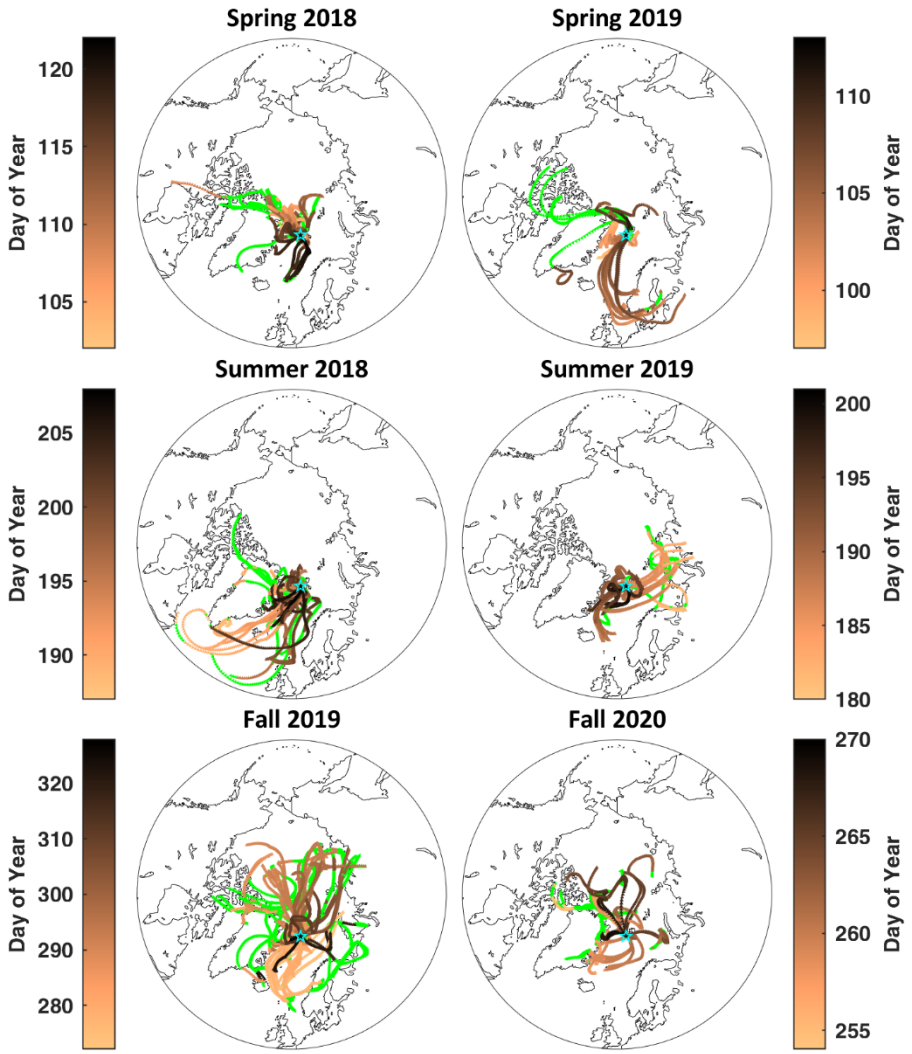

Figure S7. Back trajectories associated to the analysed samples colour-coded based on the sampling date. In dark light green are represented trajectories travelling above the planetary boundary layer height and therefore excluded from the analyses.

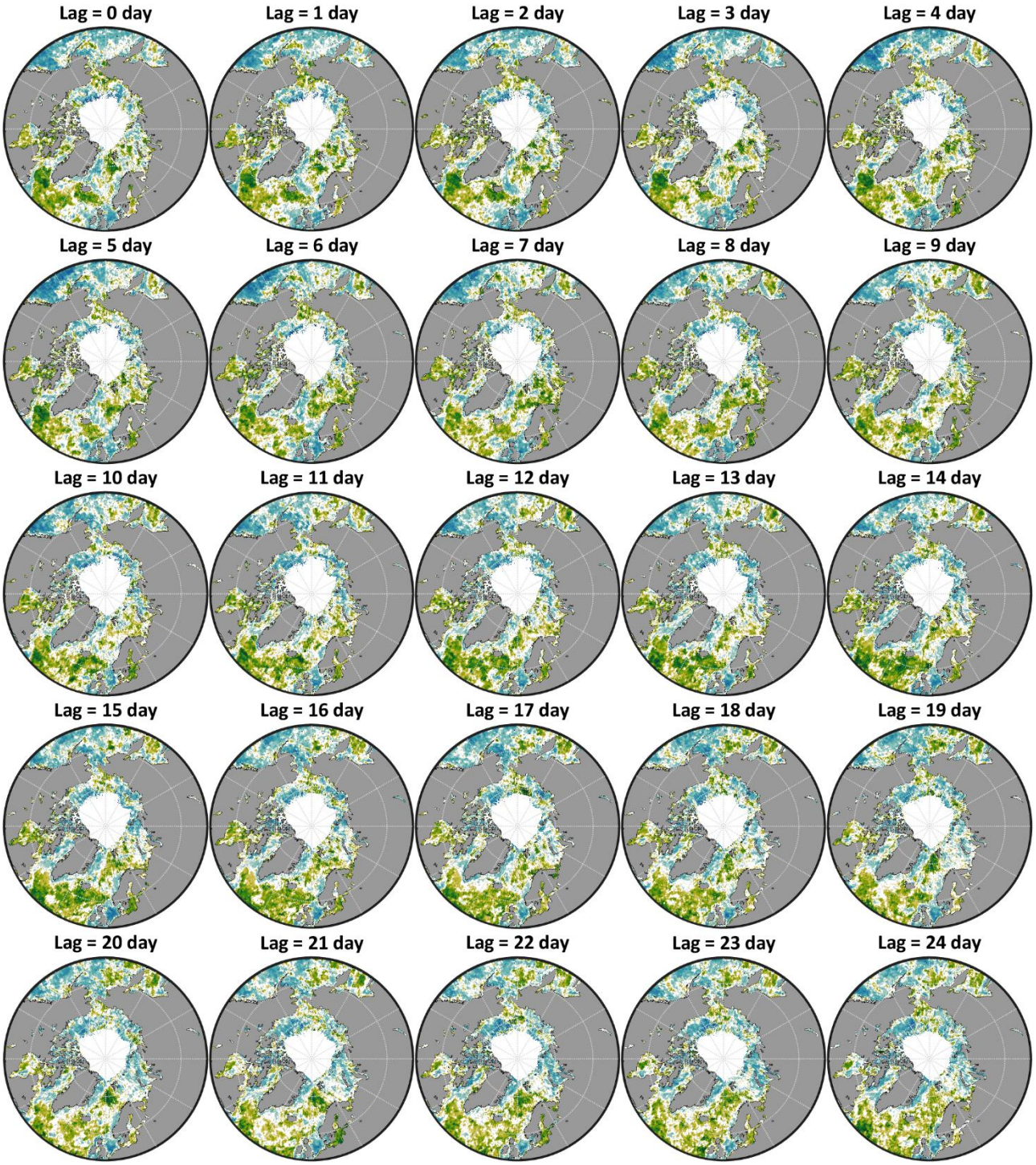

Figure S8. Spatial distribution of the correlation coefficient between nINP$_{PM1}$ [T= -15 °C] measured at GVB and CHL over the Arctic and Atlantic Ocean at different time-lags from 0 to 24 days. The grey colour represents non-significant correlation coefficients ($p<0.05$). The colour scale is the same as in Figure 9a.

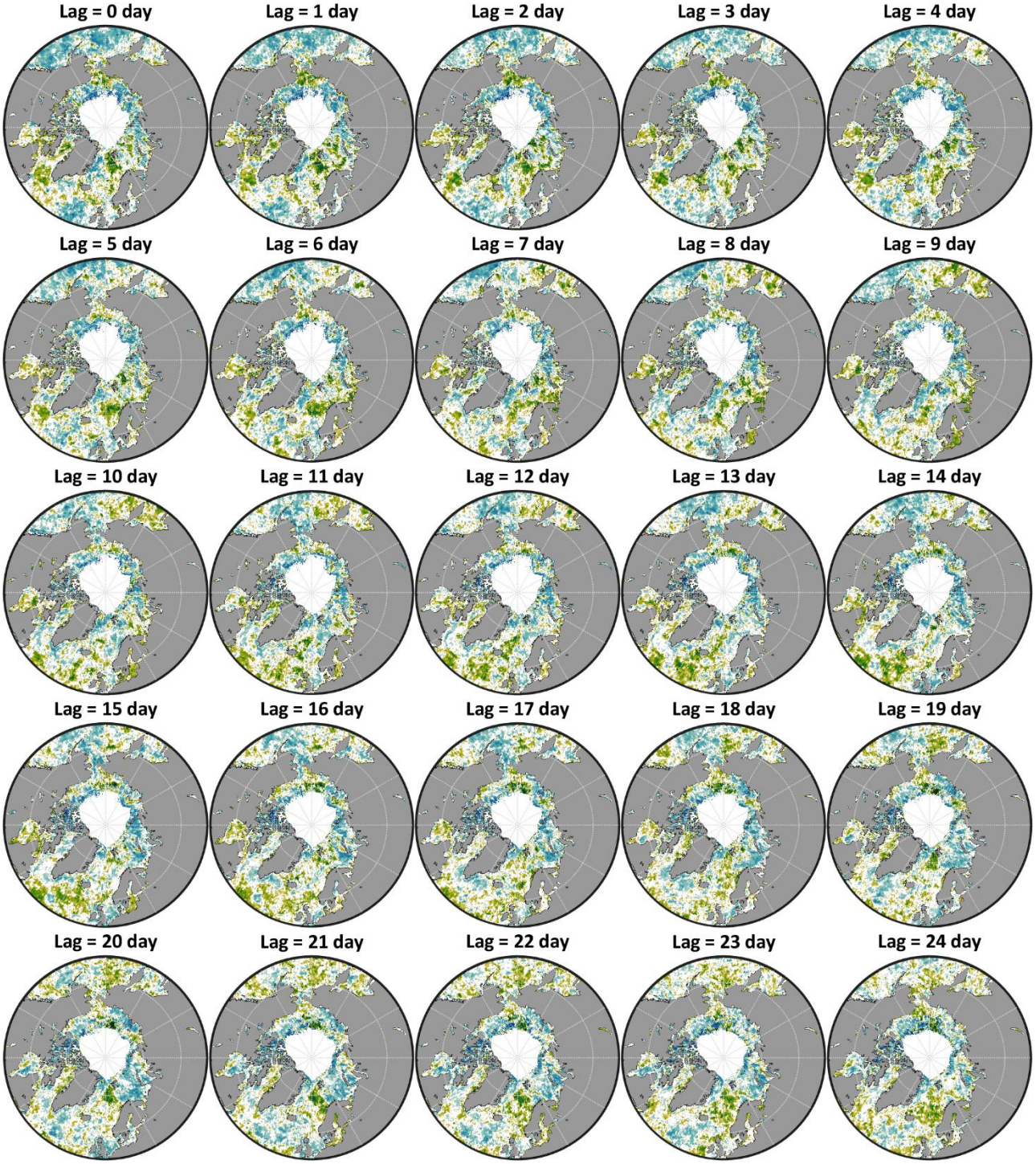

Figure S9. Spatial distribution of the correlation coefficient between nINP$_{PM1}$ [T= -18 °C] measured at GVB and CHL over the Arctic and Atlantic Ocean at different time-lags from 0 to 24 days. The grey colour represents non-significant correlation coefficients ($p<0.05$). The colour scale is the same as in Figure 9a.

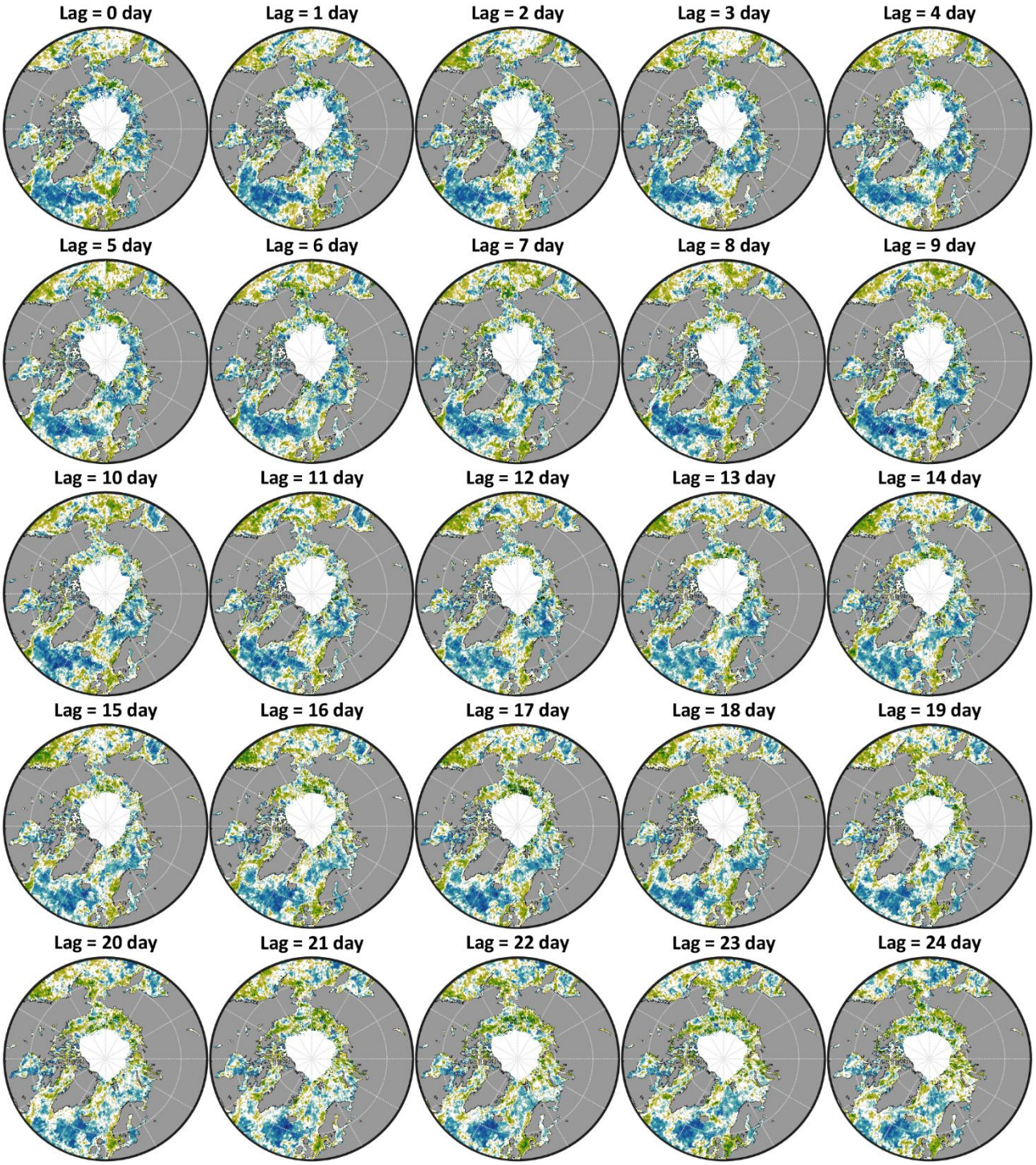

Figure S10. Spatial distribution of the correlation coefficient between $n\mathrm{INP}_{\mathrm{PM1}}$ [T= -22 °C] measured at GVB and CHL over the Arctic and Atlantic Ocean at different time-lags from 0 to 24 days. The grey colour represents non-significant correlation coefficients ($p<0.05$). The colour scale is the same as in Figure 9a.